

Invasion speeds in fluctuating environments

Michael G. Neubert^{1*}, Mark Kot² and Mark A. Lewis³

¹*Biology Department, Woods Hole Oceanographic Institution, Woods Hole, MA 02543-1049, USA*

²*Department of Mathematics and Department of Ecology and Evolutionary Biology, University of Tennessee, Knoxville, TN 37996-1300, USA*

³*Department of Mathematics, University of Utah, Salt Lake City, UT 84112, USA*

Biological invasions are increasingly frequent and have dramatic ecological and economic consequences. A key to coping with invasive species is our ability to predict their rates of spread. Traditional models of biological invasions assume that the environment is temporally constant. We examine the consequences for invasion speed of periodic and stochastic fluctuations in population growth rates and in dispersal distributions.

Keywords: invasions; variable environments; integrodifference equations

1. INTRODUCTION

Forty-two years ago, Charles Elton (1958) warned of the accelerating rate of introduction of foreign species and of the biological dislocations that follow. A recent spate of volumes on biological invasions suggests that Elton's dire predictions are coming to pass and that ecologists are having to spend more and more of their time dealing with invasions. The problem is monumental. In one recent year, 456 million exotic plants were imported into the United States (Center *et al.* 1995). These plants represent a huge pool of potential invaders, directly, through their own escape and naturalization, and indirectly, through the insects and other pathogens that they harbour. Comparable examples involving other taxa abound.

A key to coping with invasive species is the ability to predict their rates of spread (Sharov & Liebhold 1998). Improving our ability to do so, in the face of environmental fluctuations, is the goal of this article.

We model invasions with discrete-time, continuous-space, integrodifference equation (IDE) models. These models have a surprisingly long history, finding application in physics (Markoff 1912; Chandrasekhar 1943), population genetics (Slatkin 1973; Weinberger 1978), ecology (Skellam 1951; Kot & Schaffer 1986) and, as continuous-time models, in epidemiology (Mollison 1977). IDE models have become more popular recently, in part because they can incorporate a range of dispersal mechanisms (Neubert *et al.* 1995), including those that lead to the leptokurtic distributions of propagules that are common in empirical data (Okubo 1980; Kot *et al.* 1996). This is the principal advantage of IDEs over reaction-diffusion equations, which implicitly assume normal distributions.

In §2 we briefly review the simplest IDE model for invasions in a constant environment (Kot *et al.* 1996). This model has solutions called *travelling waves*—solutions with constant shape that move with a constant speed (figure 1). The speed depends on the shape of the dispersal kernel (the component of the model that describes the movement of propagules) and on the population's growth rate.

These results assume that the environment is temporally and spatially homogeneous. In fact, invading organisms regularly encounter fluctuations in environmental conditions and these translate into variation in the vital rates and/or dispersal rates (Shigesada & Kawasaki 1997). We describe the effect of temporal fluctuations in both the population growth rate and the dispersal kernel on the speed of invasion in single-species IDE models. We consider two kinds of variability: periodic (representing, for example, seasonality) and stochastic.

2. CONSTANT ENVIRONMENTS

The simplest nonlinear IDE model prescribes the population density $n_{t+1}(x)$ in the $(t + 1)$ st generation given the density in the previous generation. It takes the form

$$n_{t+1}(x) = \int_{-\infty}^{+\infty} k(x-y) f[n_t(y)] dy, \quad (1)$$

and can be understood as the composition of two temporally distinct processes: growth and dispersal.

Growth occurs during a sedentary stage, modelled using a nonlinear map such as the compensatory model

$$f[n_t(x)] = \frac{\lambda n_t(x)}{1 + \lambda n_t(x)}, \quad \lambda > 0. \quad (2)$$

In the second stage, progeny disperse. The dispersal kernel $k(x)$ is the probability density function for the distance that propagules move. The convolution operator in equation (1) tallies the movement of progeny from all y to x . We will focus our attention on thin-tailed dispersal kernels (i.e. kernels with exponentially bounded tails) such as the Gaussian, or the leptokurtic Laplace probability density function

$$k(x) = \frac{\alpha}{2} e^{-\alpha|x|}. \quad (3)$$

We touch on the effects of fat-tailed kernels (Kot *et al.* 1996) in the discussion. Neubert *et al.* (1995) describe how dispersal kernels can be derived from mechanistic models of the dispersal process.

A typical solution of the IDE (1), with an initial condition that is restricted to a finite portion of space, grows and spreads, eventually converging to a travelling wave

* Author for correspondence (mneubert@whoi.edu).

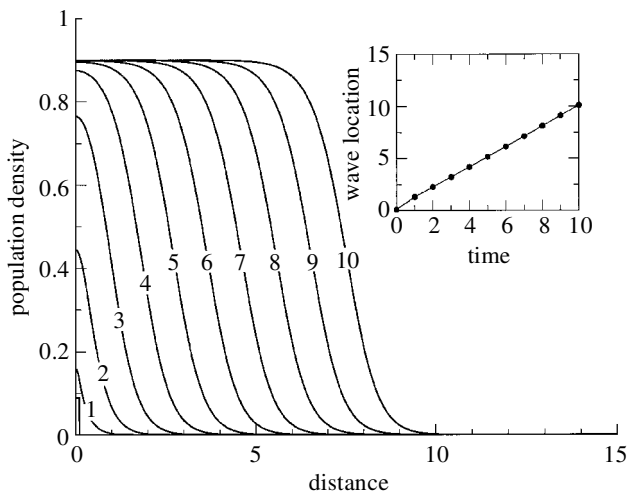


Figure 1. Travelling wave of invasion. Iterations 1–10 of the IDE model defined by equations (1)–(3). $\lambda = 10$, $\alpha = 4$.

with constant speed c (figure 1). Weinberger (1978, 1982; also see Kot *et al.* 1996; Kot 1992; Neubert & Caswell 2000) showed that for such initial conditions the eventual invasion speed is

$$c = \min_{s \in \mathcal{S}} \left\{ \frac{1}{s} \ln[\lambda m(s)] \right\}, \tag{4}$$

where $\lambda \equiv f'(0)$ is the population growth rate at low population density, $m(s) \equiv \int_{-\infty}^{+\infty} k(x)e^{sx} dx$ is the moment generating function of the kernel, and \mathcal{S} is the set of all $s > 0$ for which this integral converges (typically $[0, s_{\max}]$).

Formula (4) is correct as long as $\lambda > 1$ and the function f does not exhibit any Allee effect, i.e. as long as

$$0 \leq f(n) \leq \lambda n, \tag{5}$$

for $n \geq 0$. We will assume that inequalities (5) hold for all environmental conditions. Courchamp *et al.* (1999) and Stephens & Sutherland (1999) review the ecological causes and consequences of Allee effects.

Formula (4) also gives the speed of the slowest non-negative travelling wave solution, $n_t(x) \propto \exp[-s(x - ct)]$, to the linearization of equation (1) around $n = 0$:

$$n_{t+1}(x) = \lambda \int_{-\infty}^{+\infty} k(x - y) n_t(y) dy. \tag{6}$$

There is compelling evidence that the asymptotic speed of invasion of a nonlinear model is always the same as that of its linearization as long as there are no Allee effects, and as long as an individual only affects its environment locally (i.e. there is no long-distance density dependence). This principle has come to be known as the *linear conjecture* (Van den Bosch *et al.* 1990; Mollison 1991). (Although Allee effects are easy to detect in single-species models, see Hosono (1995) for their insidious appearance in a competition model.)

Because the linear equation (6) is easier to analyse than its nonlinear progenitor (1), we use the linear conjecture to derive speeds of invasion in fluctuating environments. Numerical simulations suggest that this at least provides a good approximation to the actual asymptotic speed. In any case, inequality (5) guarantees

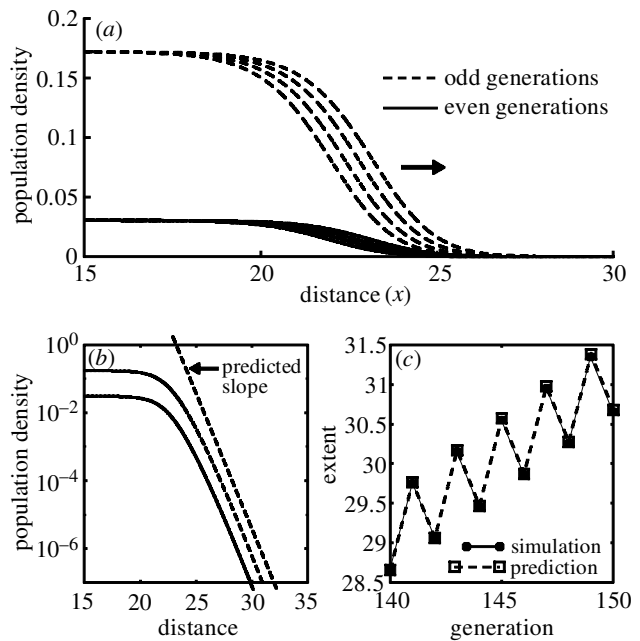


Figure 2. (a) Simulated iterations 140–150 of the periodically forced IDE defined by equations (7), (2) and (3). λ_t alternated between 6 and 0.25; α_t alternated between 4 and 6. The shape of the front in each generation (b, solid lines) and the population’s spatial extent (c, solid lines) match with predictions based on equations (9) and (10) (dashed lines).

us that the speeds we derive will be upper bounds on the actual asymptotic speed.

In simulations, we measure the speed of invasion by finding the location farthest from the origin with a population density larger than a critical density (n_{cr}) and determining how this location (x_t) changes with time. In a constant environment the shape of the invasion wave does not change, so this operational definition works as long as n_{cr} is less than the carrying capacity. In the fluctuating environments we consider next, the shape of the wave at high population densities changes between generations. We therefore require that $n_{cr} \ll 1$.

3. FLUCTUATING ENVIRONMENTS

Environmental fluctuations can be incorporated into model (1) by making the population growth rate λ and the dispersal kernel $k(x)$ functions of time (Hardin *et al.* 1988):

$$n_{t+1}(x) = \int_{-\infty}^{+\infty} k_t(x - y) f[n_t(y); \lambda_t] dy. \tag{7}$$

Using the linear conjecture, we will assume that the velocity of an invasion described by (7) is governed by its linearization around $n = 0$:

$$n_{t+1}(x) = \lambda_t \int_{-\infty}^{+\infty} k_t(x - y) n_t(y) dy. \tag{8}$$

(a) Periodic environments

To mimic the effect of a seasonal environment, we assume a periodic variation in the population growth rate (λ_t), or in the parameters of the dispersal kernel, or in both. In figure 2, we show a typical solution to model (7)

in an environment of period two. A population initially concentrated at the origin evolves into a spreading wave which alternately advances and retreats a fixed distance each generation. Every other generation, the solution looks like a travelling wave in a constant environment, having constant shape and moving with constant speed. We call such a solution a *travelling two-cycle*. We have found travelling p -cycles in this model whenever the environment fluctuates with period p .

To predict the speed of these travelling p -cycles, we have adapted a standard method for finding invasion speeds in constant environments (see Appendix A). The results are formulae for the average speed, \bar{c}_p :

$$\bar{c}_p = \min_{s \in \mathcal{S}} \left\{ \frac{1}{s} \ln \left[\prod_{i=0}^{p-1} \lambda_i m_i(s) \right]^{1/p} \right\}, \tag{9}$$

and for the instantaneous speed between generations c_i :

$$c_i = \frac{1}{\bar{s}_{\min}} \ln [\lambda_i m_i(\bar{s}_{\min})], \tag{10}$$

(figure 2). Here $m_i(s)$ is the moment generating function for $k_i(x)$, $\mathcal{S} = \bigcap_{i=0}^{p-1} \mathcal{S}_i$, and \mathcal{S}_i is the set of all $s > 0$ for which $m_i(s)$ exists. \bar{s}_{\min} , the value of s that produces the minimum in equation (9), predicts the shape of the wave; for large values of x and t , where the population density is low, $n_t(x)$ is proportional to $e^{-\bar{s}_{\min}x}$ (figure 2).

Comparing formula (9) with its constant environment analogue (4), we see that the average speed is obtained by replacing $\lambda m(s)$ in equation (4) with the geometric mean $[\prod_{i=0}^{p-1} \lambda_i m_i(s)]^{1/p}$. Geometric means will appear again when we discuss stochastic fluctuations and have important implications for predicting invasion success. In particular, if the geometric mean of the growth rates $(\prod_{i=0}^{p-1} \lambda_i)^{1/p}$ is less than unity, then $n_t \rightarrow 0$ as $t \rightarrow \infty$, the invasion fails, and formula (9) no longer applies.

Imagine environmental conditions alternating between two states as in figure 2: a good state with growth rate λ_0 and a bad state with growth rate $\lambda_1 < \lambda_0$. Using equation (10) we can calculate the instantaneous invasion speed just after a good state (c_0) and just after a bad state (c_1). Using equation (4) we can also calculate the invasion speed if the environment were always good (\hat{c}_0) or always bad (\hat{c}_1). Because

$$c_i = \frac{1}{\bar{s}_{\min}} \ln[\lambda_i m_i(\bar{s}_{\min})] > \min_{s \in \mathcal{S}_i} \left\{ \frac{1}{s} \ln[\lambda_i m_i(s)] \right\} = \hat{c}_i, \tag{11}$$

the invasion is faster after a bad state in the fluctuating environment than it would have been if conditions were always bad. It is even possible for the wave to advance after a very bad year when $\lambda_1 < 1$ (figure 3). Surprisingly, the invasion is also faster after a good state in the fluctuating environment than it would have been if conditions were always good.

Inequality (11) holds whatever the periodicity of the fluctuations; instantaneous speeds in fluctuating environments are always greater than the comparable speeds in the component constant environments.

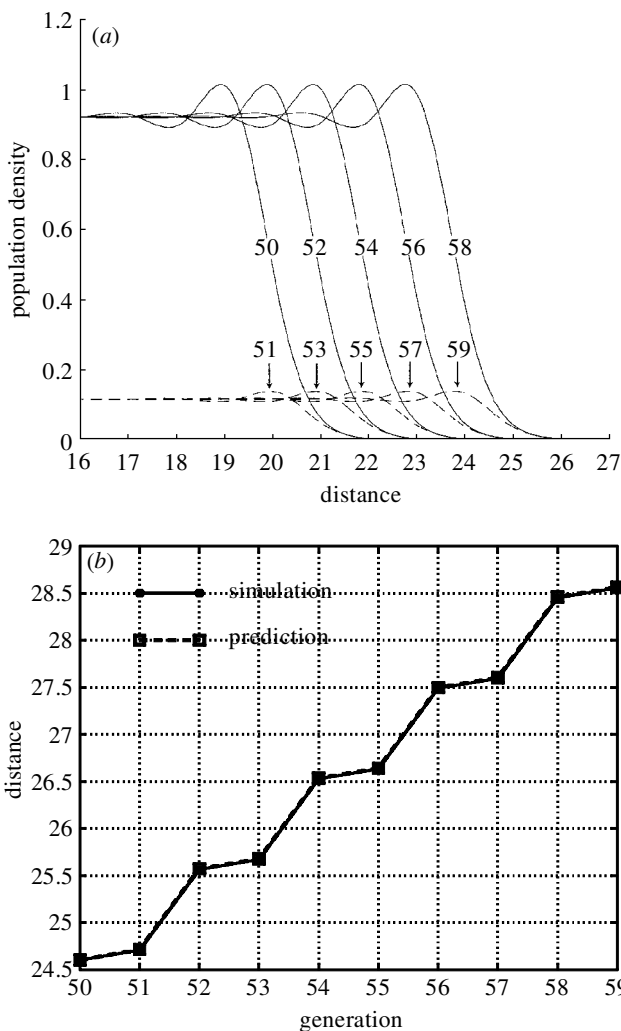


Figure 3. (a) Simulation of model (7) and (3) with the overcompensatory growth function and $f = \lambda_t n_t \exp(-n_t)$. $\alpha_0 = \alpha_1 = 5$ with $\lambda_0 = 10$ and $\lambda_1 = 0.8$. (b) Predictions (based on equations (9) and (10)) that the wave will advance even after a bad year agree with the numerical simulation.

(b) *Stochastic environments*

Real environmental fluctuations include both stochastic and periodic components. Environmental stochasticity can be incorporated by choosing the growth rates and dispersal kernels at random from a set of choices. Model (7) then becomes

$$N_{t+1}(x) = \int_{-\infty}^{+\infty} K_t(x-y) f[N_t(y); \Lambda_t] dy, \tag{12}$$

where $K_t(x)$ are independent and identically distributed (iid) random dispersal kernels, and the growth rates Λ_t are iid random variables independent of the kernels. (More generally, we conjecture that the results of this section will also hold if $K_t(x)$ and Λ_t are governed by stationary ergodic stochastic processes.) The linearization of equation (12) is

$$N_{t+1}(x) = \Lambda_t \int_{-\infty}^{+\infty} K_t(x-y) N_t(y) dy. \tag{13}$$

We again assume that the linearization governs the speed of the nonlinear model.

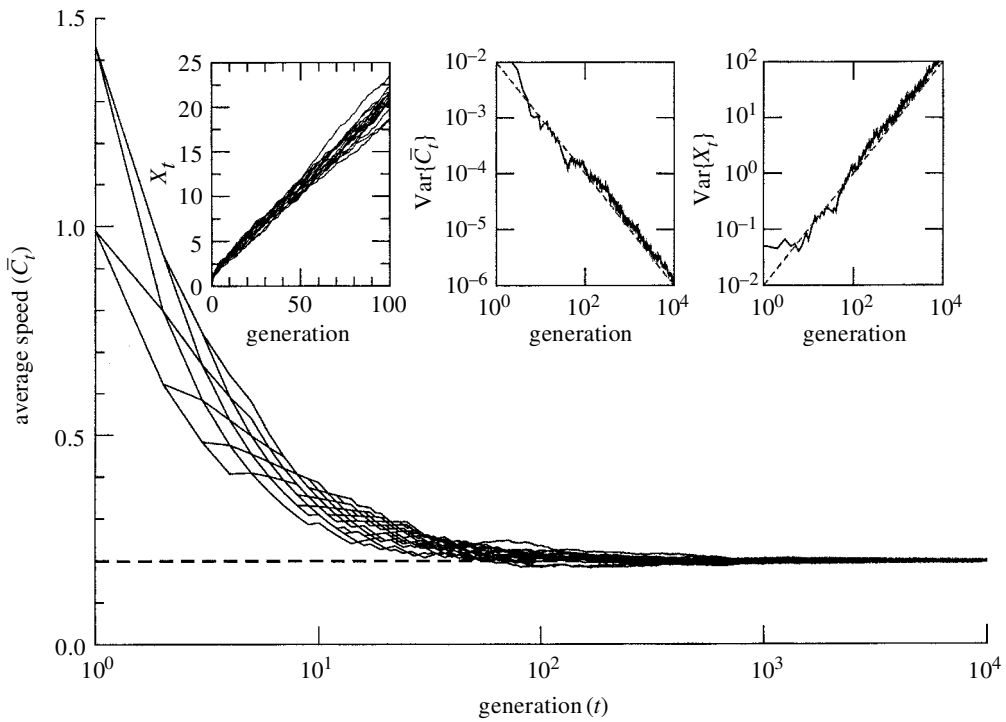


Figure 4. Twenty realizations of the stochastic model defined by equations (12), (2) and (3). At each time the parameter pair (λ_t, α_t) was chosen at random from the set $\{(1.10, 6.0), (1.35, 4.0)\}$. $n_{cr} = 10^{-6}$. The predicted average asymptotic speed (\bar{c}) is shown with a dashed line. Insets, (left) spatial extent of the 20 realizations; (middle) $\text{Var}[\bar{C}_t]$ (solid line) decays like $1/t$ (dashed line); (right) $\text{Var}[X_t]$ (solid line) grows like t (dashed line).

The population densities $N_i(x)$ are now random variables. Taking expectations in equation (13) we have

$$E[N_{t+1}(x)] = E[\Lambda_t] \int_{-\infty}^{+\infty} E[K_t(x-y)] E[N_t(y)] dy, \quad (14)$$

a deterministic IDE for the expected population density. Formula (4) applies and the velocity (\bar{c}) with which the expected value of $N_t(x)$ expands is

$$\bar{c} = \min_{s \in S} \left\{ \frac{1}{s} \ln (E[\Lambda_0] E[M_0(s)]) \right\}. \quad (15)$$

Thus the average population asymptotically spreads at a rate determined by the average environmental conditions, i.e. the average growth rate and the average kernel. If dispersal and growth are correlated, equation (15) becomes

$$\bar{c} = \min_{s \in S} \left\{ \frac{1}{s} \ln (E[\Lambda_0 M_0(s)]) \right\}.$$

Positive correlations will increase \bar{c} .

Consider, however, that at any time t the population has a random extent X_t , defined to be the location farthest from the invasion's origin with $N_t(x) \geq n_{cr}$. The average speed since the invasion began is therefore also a random variable, given by $\bar{C}_t \equiv (X_t - x_0)/t$. As we show in Appendix A, \bar{C}_t is asymptotically normally distributed with mean (μ) and variance (σ^2) given by

$$\mu = \min_{s \in S} E \left[\frac{\ln (\Lambda_0 M_0(s))}{s} \right], \quad (16a)$$

$$\sigma^2 = \frac{1}{t} \text{Var} \left[\frac{\ln (\Lambda_0 M_0(s^*))}{s^*} \right], \quad (16b)$$

where s^* is the value of s that gives the minimum for μ . As $t \rightarrow \infty$, the variance decays to zero and $\bar{C}_t \rightarrow \bar{c}$ in probability where

$$\bar{c} = \min_{s \in S} \left\{ \frac{1}{s} E[\ln (\Lambda_0 M_0(s))] \right\}. \quad (17)$$

Since the expectation of the logarithm of a random variable is equal to the logarithm of its geometric mean, we have, as in the periodic case, replaced the product $\lambda m(s)$ in formula (4) with the geometric mean of this quantity. Note that $\bar{c}_p \rightarrow \bar{c}$ as the environmental periodicity $p \rightarrow \infty$, and that the formula for \bar{c} reduces to the formula for \bar{c}_p when the environment is periodic.

By equations (16), the probability of observing an average speed other than \bar{c} is asymptotically zero. Since $E[\ln (\lambda_0 M_0(s))] < \ln \{E[\lambda_0] E[M_0(s)]\}$, $\bar{c} < \bar{c}$; as $t \rightarrow \infty$, the average population spreads faster than almost every realization of the process. In particular, it is possible for \bar{c} to be positive and \bar{c} to be negative, in which case the invasion certainly fails, even though it would succeed in a constant 'average' environment.

Figure 4 shows \bar{C}_t versus t for twenty realizations of model (12). While each realization converges to the predicted average asymptotic speed \bar{c} , it should be noted that the spatial extent of a realized invasion does *not* converge to $\bar{c}t$ (figure 4). Assume, without loss of generality, that $x_0 = 0$. Then, since $X_t = t\bar{C}_t$, $\text{Var}[X_t] = t^2 \text{Var}[\bar{C}_t] = t\sigma^2$ (cf. equations (16)). Thus the variance in extent grows linearly with time (figure 4).

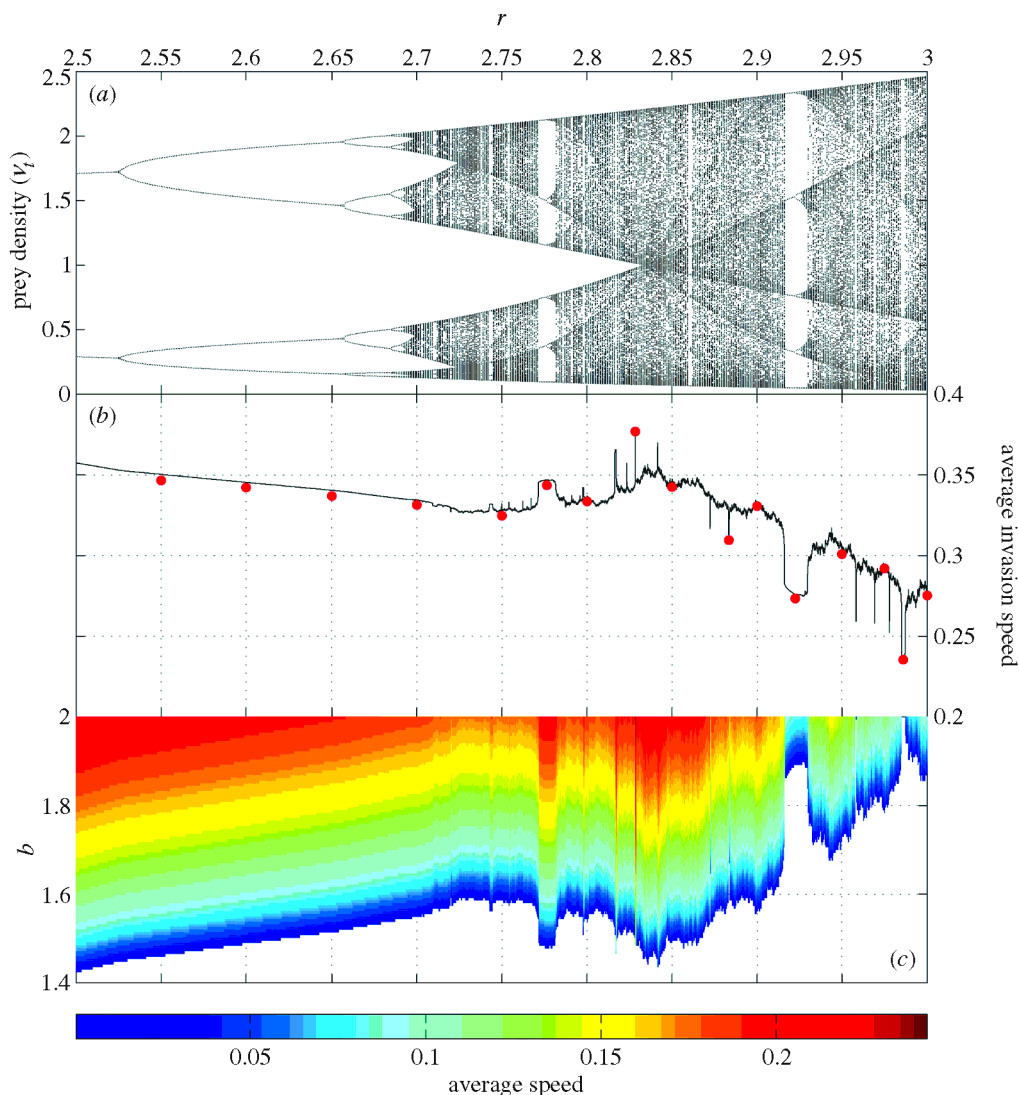


Figure 5. Predator invading a fluctuating prey population. (a) Asymptotic prey dynamics in the absence of the predator. (b) Speeds of predator invasion based on simulations of model (18) with $b = 3.2$ (dots) match the predictions based on formula (17) (solid line). Prey do not disperse; predators have a Laplace dispersal kernel with $\alpha = 5.85$. (c) Average predator invasion speed as a function of r and b . A small predator invasion fails in the white region.

4. DISCUSSION

(a) Predator invasions

One important source of environmental variability is an organism’s food supply. For example, consider a predator (n) invading a population of its prey (v), which has been established long enough to exhibit its asymptotic dynamics—a situation typical of biological invasions and of many biological control scenarios. A simple IDE model for this system is

$$v_{t+1}(x) = \int_{-\infty}^{+\infty} h(x-y) v_t(y) \exp\{r[1 - v_t(y) - n_t(y)]\} dy, \tag{18a}$$

$$n_{t+1}(x) = \int_{-\infty}^{+\infty} k(x-y) b v_t(y) n_t(y) dy, \tag{18b}$$

(Neubert *et al.* 1995; Neubert & Kot 1992). We can use our theory to predict the predator’s invasion speed.

We begin, in the absence of the predator, with the prey uniformly distributed in space and either at equilibrium,

cycling periodically, or chaotic, depending on the value of r (figure 5a). Call this solution $v_t(x) = v_t$.

The predator is introduced at low density in a small region of space. Its growth rate at time t is $bv_t(x)$; fluctuations in prey population size translate into fluctuations in the predator growth rate. Far in front of the predator wave, predators have a negligible effect on the prey and $v_t(x) \approx v_t$. We therefore use formula (17) for the predator’s invasion speed, using the moment generating function of $k(x)$ for $M_0(s)$ and replacing Λ_0 with bv_t . Figure 5b shows the invasion speed based on equation (17) for various values of the prey growth rate r . Superimposed on the curve are the results of numerical simulations.

Figure 5 shows that formula (17) is accurate not only when environmental fluctuations are periodic or stochastic, but also when they are chaotic. Small changes in parameters can cause large changes in the geometric mean growth rate, and hence in invasion speed. The direction of such changes may not be obvious. In model (18), as the growth rate of the prey is increased, the

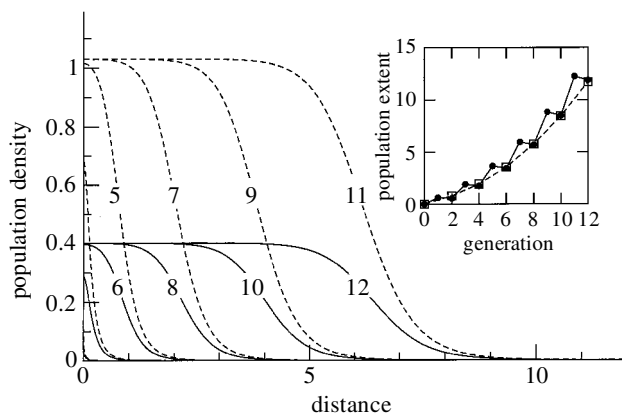


Figure 6. An accelerating invasion in a periodic environment (circles, simulation; squares, prediction for t even). The model defined by (7), (2) and the fat-tailed kernel $k_t(x) = (\beta_t^2/4)\exp[-\beta_t\sqrt{|x|}]$ was simulated from an inoculum at the origin. λ_t alternated between 200 and 0.5; β_t alternated between 7 and 10.

predator invasion tends to slow down, in some cases even reversing direction.

In figure 5c we extrapolate the predicted speed to other values of b . For parameter values in the white region, a locally stable, spatially homogeneous equilibrium with positive predator and prey densities coexists with a prey-only attractor (Neubert & Kot 1992). This effectively creates an Allee effect, for the predator. In the white region, a small predator inoculum will not invade the prey, but a large enough inoculum will initiate an invasion. Because of this Allee effect the linear conjecture no longer holds and formula (17) does not apply. The invasion is no longer ‘pulled’ by the leading edge of the wave, but is ‘pushed’ by individuals reproducing at high densities and spilling outward (via dispersal) at densities sufficient to overcome the threshold for population growth (Kot *et al.* 1996).

(b) Fat-tailed kernels

So far, we have discussed dispersal kernels with tails that decay at least exponentially fast. Recently, interest has developed in ‘fat-tailed kernels’, with tails that decay slower than exponentially. These kernels capture the prevalence of long-distance dispersal events and the surprising rapidity of some invasions (Clark *et al.* 1998). Minogue (1989), Shaw (1994) and Kot *et al.* (1996) discuss the importance of long-distance dispersal to the population dynamics of plant pathogens, and list many examples.

Fat-tailed kernels in constant environments are known to convert constant speed travelling wave solutions into accelerating waves (Kot *et al.* 1996). The same effect occurs in fluctuating environments. In figure 6 we show the extent of a typical solution to model (7) with a fat-tailed kernel in an environment with period 2. The population evolves into a spreading wave, but now the wave advances (and retreats) a larger distance with each time-step.

Viewed every other generation, the solution looks like the typical accelerating wave in a constant environment. Building on this observation, we modified the method of Kot *et al.* (1996) to predict the wave’s location (x_{ip}) every p -generations in p -periodic environments. Using the notation ‘ \circ ’ for the convolution operator and defining

$k^{(p)}(x) \equiv k_0(x) \circ k_1(x) \circ \dots \circ k_{p-1}(x)$, the result is given (implicitly) by

$$n_{cr} = n_0 \left(\prod_{i=0}^{p-1} \lambda_i \right)^t k^{(p)}(x_{ip}). \tag{19}$$

This result holds as long as $k^{(p)}(x)$ has moments of all orders and tails that are sufficiently flat (see Kot *et al.* 1996, equation (A.27)). The prediction based on equation (19) agrees with numerical simulations (figure 6).

(c) Arithmetic versus geometric means

The formulae for invasion speeds in both periodic and stochastic environments are similar to the constant environment formula: the product $\lambda m(s)$ in equation (4) is replaced by its geometric mean. Because the geometric mean is less than the arithmetic mean, with probability 1, a realization of the stochastic invasion process (12) eventually spreads more slowly than the expected population. For the same reason, the speed of invasion in a periodic environment is slower than if the invasion had occurred in an average constant environment.

The importance of the distinction between geometric and arithmetic means in population biology was first pointed out by Lewontin & Cohen (1969). They showed that in the non-spatial model, $N_{t+1} = \Lambda_t N_t$, the expected population grows faster (at the rate $\ln E[\Lambda_0]$) than almost every realization of the process (which grow at the rate $E[\ln \Lambda_0]$). This difference is to be expected in any multiplicative process such as population growth (Cohen 1979; Tuljapurkar 1982). Lewontin & Cohen (1969) also showed that the discrepancy between geometric and arithmetic means disappears in continuous-time models. It is straightforward to show that, in contrast to IDEs, the speed of the expectation is the same as the expectation of the speed in single-species reaction–diffusion models when the intrinsic growth rate and the diffusion coefficient are continuous functions that vary randomly with time.

Supported by grants from the National Science Foundation (DEB-9527400, DMS-9973212, DMS-9457816) and a Texaco Research Award in Science, Technology, and Public Policy to M.G.N. Discussions with H. Caswell, A. Solow, and P. van den Driessche improved the manuscript. Woods Hole Oceanographic Institution contribution no. 10227.

APPENDIX A

We begin by finding the average speed of invasion for model (7) for any deterministic sequence of growth rates and dispersal kernels. Using the linear conjecture, we look for exponential solutions to equation (8). Given that

$$n_0(x) = a \exp(-sx), \tag{A1}$$

the solution to equation (8) is

$$n_t(x) = a \left\{ \prod_{i=0}^{t-1} \lambda_i m_i(s) \right\} \exp(-sx). \tag{A2}$$

From equation (A1),

$$n_{cr} = a \exp(-sx_0), \tag{A3}$$

and from equation (A2)

$$n_{cr} = a \left\{ \prod_{i=0}^{t-1} \lambda_i m_i(s) \right\} \exp(-sx_t). \quad (A4)$$

Dividing equation (A4) by equation (A3), we can solve for the average speed between the initial time and time t :

$$\bar{c}_t(s) \equiv \frac{x_t - x_0}{t} = \frac{1}{s} \ln \left[\left(\prod_{i=0}^{t-1} \lambda_i m_i(s) \right)^{1/t} \right]. \quad (A5)$$

Condition (5) ensures that the linearization (8) gives an upper bound on the invasion speed of (7). For initial conditions with compact support we can assume that $n_0(x) \leq a \exp(-sx)$.

Then by equation (8),

$$n_1(x) \leq \lambda_0 m_0(s) a \exp(-sx) = a \exp\{-s[x - \bar{c}_1(s)]\}. \quad (A6)$$

Plugging (A6) into (8) gives

$$n_2(x) \leq \lambda_1 m_1(s) a \exp\{-s[x - \bar{c}_1(s)]\} = a \exp\{-s[x - 2\bar{c}_2(s)]\}. \quad (A7)$$

Continuing in this fashion we find $n_t(x) \leq a \exp\{-s[x - t\bar{c}_t(s)]\}$. Thus $\bar{c}_t(s)$ is an upper bound on the average rate of spread to time t . Because we are free to adjust the constant a , we can use any $s > 0$ for which all the $m_i(s)$ exist (i.e. $s \in \mathcal{S}$). Minimizing $\bar{c}_t(s)$ with respect to s gives

$$\bar{c}_t = \min_{s \in \mathcal{S}} \left\{ \frac{1}{s} \ln \left[\left(\prod_{i=0}^{t-1} \lambda_i m_i(s) \right)^{1/t} \right] \right\}. \quad (A8)$$

(a) Periodic fluctuations

In the case of periodic fluctuations the average speed, as $t \rightarrow \infty$, is found by replacing t in equation (A8) by the period p . The result is equation (9).

(b) Stochastic fluctuations

Assume that each of the growth rates λ_i is a realization of a random variable Λ_i , and that the Λ_i are independent and identically distributed (iid). Similarly, assume that the $k_i(x)$ are realizations of the iid random variables $K_i(x)$, and that $M_i(s)$ and $m_i(s)$ are the moment generating functions of $K_i(x)$ and $k_i(x)$ respectively.

The population density $N_t(x)$ and the population extent X_t are random variables. In this case

$$\bar{C}_t(s) \equiv \frac{X_t - x_0}{t}, \quad (A9a)$$

$$= \frac{1}{s} \ln \left[\left(\prod_{i=0}^{t-1} \Lambda_i M_i(s) \right)^{1/t} \right], \quad (A9b)$$

$$= \frac{1}{t} \sum_{i=0}^{t-1} \frac{1}{s} \ln[\Lambda_i M_i(s)]. \quad (A9c)$$

For any s , equation (A9c) states that $\bar{C}_t(s)$ is the sample mean of $\{\ln[\Lambda_i M_i(s)]\}/s$ up to time t . If the $\Lambda_i M_i(s)$ terms are iid with finite expectation and variance, then the $\{\ln[\Lambda_i M_i(s)]\}/s$ terms also have finite expectation $\mu(s) = E\{\ln[\Lambda_0 M_0(s)]\}/s$ and finite

variance $\sigma^2(s) = \text{Var}\{\ln[\Lambda_0 M_0(s)]/s\}$. By the central limit theorem, $\bar{C}_t(s)$ is approximately normally distributed with mean $\mu(s)$ and variance $[\sigma^2(s)]/t$.

Because our initial conditions have compact support, we can use any $s \in \mathcal{S}$, including the value of s that minimizes $\mu(s)$. Call this value s^* . Thus, $\bar{C}_t \equiv \bar{C}_t(s^*)$, is approximately normally distributed with mean and variance given by equation (16).

REFERENCES

Center, T. D., Frank, J. H. and Dray, F. A. 1995 Biological invasions: stemming the tide in Florida. *Florida Entomol.* **78**, 45–55.

Chandrasekhar, S. 1943 Stochastic problems in physics and astronomy. *Rev. Mod. Phys.* **15**, 1–91.

Clark, J. S. (and 12 others) 1998 Reid’s paradox of rapid plant migration. *BioScience* **48**, 13–24.

Cohen, J. E. 1979 Comparative statics and stochastic dynamics of age-structured populations. *Theor. Popul. Biol.* **16**, 159–171.

Courchamp, F., Clutton-Brock, T. and Grenfell, B. 1999 Inverse density dependence and the Allee effect. *Trends Ecol. Evol.* **14**, 405–410.

Elton, C. S. 1958 *The ecology of invasions by animals and plants*. London: Methuen.

Hardin, D. P., Takac, P. & Webb, G. F. 1988 Asymptotic properties of a continuous-space discrete-time population model in a random environment. *J. Math. Biol.* **26**, 361–374.

Hosono, Y. 1995 Travelling waves for a diffusive Lotka–Volterra competition model. II. A geometric approach. *Forma* **10**, 235–257.

Kot, M. 1992 Discrete-time travelling waves: ecological examples. *J. Math. Biol.* **30**, 413–436.

Kot, M. & Schaffer, W. M. 1986 Discrete-time growth-dispersal models. *Math. Biosci.* **80**, 109–136.

Kot, M., Lewis, M. A. & Van den Driessche, P. 1996 Dispersal data and the spread of invading organisms. *Ecology* **77**, 2027–2042.

Lewontin, R. C. & Cohen, D. 1969 On population growth in a randomly varying environment. *Proc. Natl Acad. Sci. USA* **62**, 1056–1060.

Markoff, A. A. 1912 *Wahrscheinlichkeitsrechnung* Leipzig, Germany: Teubner.

Minogue, K. P. 1989 Diffusion and spatial probability models for disease spread. In *Spatial components of plant disease epidemics* (ed. M. J. Jeger), pp. 127–143. Englewood Cliffs, NJ: Prentice Hall.

Mollison, D. 1977 Spatial contact models for ecological and epidemic spread. *J. R. Statist. Soc. B* **39**, 283–326.

Mollison, D. 1991 Dependence of epidemic and population velocities on basic parameters. *Math. Biosci.* **107**, 255–287.

Neubert, M. G. & Caswell, H. 2000 Dispersal and demography: calculation and sensitivity analysis of invasion speed for structured populations. *Ecology* **81**, 1613–1628.

Neubert, M. G. & Kot, M. 1992 The subcritical collapse of predator populations in discrete-time predator–prey models. *Math. Biosci.* **110**, 45–66.

Neubert, M. G., Kot, M. & Lewis, M. A. 1995 Dispersal and pattern formation in a discrete-time predator–prey model. *Theor. Popul. Biol.* **48**, 7–43.

Okubo, A. 1980 *Diffusion and ecological problems: mathematical models*. Berlin: Springer-Verlag.

Sharov, A. A. & Liebhold, A. M. 1998 Bioeconomics of managing the spread of exotic pest species with barrier zones. *Ecol. Appl.* **8**, 833–845.

Shaw, M. 1994 Modeling stochastic processes in plant pathology. *A. Rev. Phytopathol.* **32**, 523–544.

- Shigesada, N. & Kawasaki, K. 1997 *Biological invasions: theory and practice*. Oxford University Press.
- Skellam, J. G. 1951 Random dispersal in theoretical populations. *Biometrika* **38**, 196–218.
- Slatkin, M. 1973 Gene flow and selection in a cline. *Genetics* **75**, 733–756.
- Stephens, P. A. and Sutherland, W. J. 1999 Consequences of the Allee effect for behaviour, ecology and conservation. *Trends Ecol. Evol.* **14**, 401–405.
- Tuljapurkar, S. D. 1982 Population dynamics in variable environments. II. Correlated environments, sensitivity analysis and dynamics. *Theor. Popul. Biol.* **21**, 114–140.
- Van den Bosch, F., Metz, J. A. J. & Diekmann, O. 1990 The velocity of spatial population expansion. *J. Math. Biol.* **28**, 529–565.
- Weinberger, H. F. 1978 Asymptotic behavior of a model of population genetics. In *Nonlinear partial differential equations and applications. Lecture notes in mathematics*, vol. 648 (ed. J. Chadam), pp. 47–98. Berlin: Springer-Verlag.
- Weinberger, H. F. 1982 Long-time behavior of a class of biological models. *SIAM J. Math. Anal.* **13**, 353–396.

As this paper exceeds the maximum length normally permitted, the authors have agreed to contribute to production costs.